Generalized Unbiased Scene Graph Generation

Xinyu Lyu, Lianli Gao, Junlin Xie, Pengpeng Zeng, Yulu Tian, Jie Shao, Heng Tao Shen *Fellow, IEEE*

***Abstract*—Existing Unbiased Scene Graph Generation (USGG) methods only focus on addressing the predicate-level imbalance that high-frequency classes dominate predictions of rare ones, while overlooking the concept-level imbalance. Actually, even if predicates themselves are balanced, there is still a significant concept-imbalance within them due to the long-tailed distribution of contexts (i.e., subject-object combinations). This concept-level imbalance poses a more pervasive and challenging issue compared to the predicate-level imbalance since subject-object pairs are inherently complex in combinations. Hence, we introduce a novel research problem: Generalized Unbiased Scene Graph Generation (G-USGG), which takes into account both predicate-level and concept-level imbalance. To the end, we propose the Multi-Concept Learning (MCL) framework, which ensures a balanced learning process across rare/ uncommon/ common concepts. MCL first quantifies the concept-level imbalance across predicates in terms of different amounts of concepts, representing as multiple concept-prototypes within the same class. It then effectively learns concept-prototypes by applying the Concept Regularization (CR) technique. Furthermore, to achieve balanced learning over different concepts, we introduce the Balanced Prototypical Memory (BPM), which guides SGG models to generate balanced representations for concept-prototypes. Finally, we introduce a novel metric, mean Context Recall (mCR@K), as a complement to mean Recall (mR@K), to evaluate the model's performance across concepts (determined by contexts) within the same predicate. Extensive experiments demonstrate the remarkable efficacy of our model-agnostic strategy in enhancing the performance of benchmark models on both VG-SGG and OI-SGG datasets, leading to new state-of-the-art achievements in two key aspects: predicate-level unbiased relation recognition and concept-level compositional generability.**

***Index Terms*—Scene graph generation, debasing, prototypical learning, memory-based learning.**

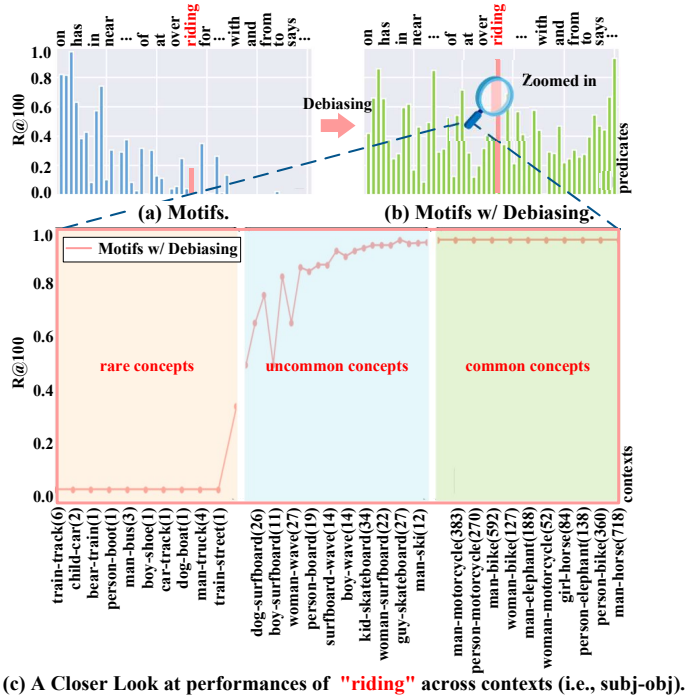

(c) A Closer Look at performances of "riding" across contexts (i.e., subj-obj).

Fig. 1. **The illustration of concept-level imbalanced predictions of Unbiased SGG methods [1]. Up:** performance (R@100) of Motifs (baseline) and Motifs w/ Debiasing across different predicates. **Down:** performance (R@100) of Motifs w/ Debiasing across different contexts (i.e., combinations between subjects & objects) within predicates "riding". (a) and (b) illustrate that Motifs w/ Debasing achieves predicate-level balanced relation recognition. Moreover, (b) and (c) demonstrate that the Debiasing method fails to attain concept-level balanced predictions across contexts within "riding".

I. Introduction

SCENE Graph Generation (SGG) plays a crucial role in providing structured representations for semantic-aligned multimodal tasks, effectively bridging the semantic gap in multimodal learning. In recent years, SGG has gained widespread popularity and application in various vision and language (VL) downstream tasks, such as VL Foundation Model Pretraining [1]–[3], Image-Text Retrieval [4]–[6], Visual Question Answering [7]–[9], and Image Synthesis [10]–[12].

Most of the existing SGG methods follow a compositional learning pipeline that detects entities (objects and subjects) and predicts pairwise relations in the form of "subject-predicate-object" triples. However, due to the long-tailed distribution across predicates, conventional SGG methods are heavily suffered from the predicate-level imbalance issue. This results in their biased predictions on relation recognition, favoring general predicates that are more frequent in the dataset, while overlooking the fine-grained predicates with lower frequency. To address the issue, several SGG debiasing methods [13]–[17] have been proposed utilizing balanced learning strategies for achieving the Unbiased Scene Graph Generation (USGG). Despite their encouraging progress on the predicate-level USGG, they neglect the exhaustive concept-level imbalance within predicates, i.e., USGG models cannot generalize well across rare/ uncommon/ common concepts. To be specific, the concept-level imbalance arises from the long-tailed distribution of contexts[1] within predicates. As shown in Fig. 1 (c), Motifs w/ Debiasing has superior performance on "man-riding-horse/ person-riding-elephant" (a common concept of "riding" with $718/138$ samples), but behaves extremely bad on "train-riding-street/ train-riding-track" (a rare concept of "riding" with $1/6$ samples).

Note that the concept-level imbalance is more pervasive and challenging compared to the predicate-level imbalance for two

Xinyu Lyu, Junlin Xie, Lianli Gao, Pengpeng Zeng, Jie Shao, Heng Tao Shen are with the Center for Future Media and School of Computer Science and Engineering, University of Electronic Science and Technology of China, Chengdu, China, 611731. Yulu Tian is with Ant Group. Corresponding author: Lianli Gao. E-mail: lianli.gao@uestc.edu.cn

[1]Defined as the subject-object pair within a relationship triple throughout the paper, following the convention established in previous works [18], [19].

main reasons: 1) Current SGG models **fail to distinguish and capture the variation across concepts within the predicates** during training. To be specific, a few common concepts contribute to most of the observations, while a large number of rare/ uncommon ones are under-represented. As a consequence, existing metric-based (i.e., predicate-level single prototype [20]–[23]) and classifier-based SGG methods (i.e., class-wise decision boundary [13], [17], [24], [25]) tend to **focus solely on handling these common concepts, leaving rare/ uncommon concepts unexplored**. However, these rare/ uncommon concepts constitute the majority of semantics within predicates, hence posing challenges to the compositional generability (i.e., referring to the model's capability to generalize across contexts) of existing SGG methods. 2) The concept-level imbalance cannot be effectively solved by directly applying the **distribution-based inductive bias (i.e., rebalancing-based prior optimization** [1], [15], [26]–[28] or **statistics-based posterior regularization** [29], [30]. On one hand, the inherently high complexity of subject-object combinations (e.g., around 27K types of triplets in VG-SGG) within predicates makes it **impractical to manually curate and balance** the dataset at the concept level, as the costly but low-yield data-augmentation-based rebalancing strategies proposed in [14], [31], [32]. On the other hand, the compositional generability necessitates SGG models to understand and infer relationships in contexts of rare or unseen subject-object combinations, which **cannot be achieved by relying on observed statistics** that are dominated by common subject-object pairs (e.g., Frequency bias in [29], Confusion Matrix in [16], and Predicate Lattice in [19]).

Therefore, in this paper, we present a new research problem, namely Generalized Unbiased Scene Graph (G-USGG), to jointly consider model's predicate-level and concept-level imbalanced predictions. To address the issue, we propose **M**ulti-**C**oncept **L**earning (MCL), a first, unified predicate-level and concept-level balanced learning framework orthogonal to existing SGG methods. The main idea behind our MCL is to enable the SGG model to **effectively capture the variation of concepts, represent and learn diverse concepts within the same class in a balanced manner** during training. To achieve that, we first propose the **Concept-Prototype Construction (CPC)** to assess predicates' semantic scales (i.e., the indicator for amounts of concepts), and then quantify the semantic scales into different amounts of concept-prototypes in a single class. To effectively learning these concepts, the **Concept Regularization (CR)** is proposed to assist SGG models in mitigating the predicate-level semantic overlap, and meanwhile enhancing the discriminability among concept-prototypes. Moreover, the **Balanced Prototypical Memory (BPM)** is developed to store balanced prototypical representations of diverse concepts. It acts as reference points, allowing SGG models to focus equally on all concepts during training, regardless of their frequency or rarity in the dataset. Finally, we propose a novel metric called **mean Context Recall (mCR)** as a complement to the traditional mean Recall (mR) metric, allowing us to evaluate model's performance across concepts. An overview of our MCL is shown in Fig. 2.

Generalizability and Strong performance: The proposed MCL can be seamlessly integrated into existing SGG methods, relieving predicate-level and concept-level imbalance issues, thus enhancing models' unbiased relation recognition capability and their compositional generalizability, respectively. On the VG-SGG dataset, when applying MCL to various benchmark models, our approach achieves average improvements of **20.9%** to **25.1%** of F@K (a harmonic average of R@K and mR@K in [14]) (Tab. I), **1.6%** to **6.6%** and **16.3%** to **16.8%** in Few-shot and Zero-shot Recall compared to baselines (Tab. III and Tab. IV). In particular, when addressing the issue of predicate-level biased predictions, MCL outperforms the state-of-the-art Inf [24] and IETrans [14] by **7.1%/ 11.2%** and **4.1%/ 10.0%** in R@100/ mR@100 of the Predcls task (Tab. I). Furthermore, after solving the concept-level imbalance problem, the MCL outperforms the state-of-the-art SQUAT [33] and PENET [20] baselines by **4.9%** and **6.6%** in FsR@100 (Few-shot Recall) (Tab. III), by **18.5%** and **1.4%** of ZsR@100 (Zero-shot Recall) (Tab. IV) of the Predcls task, respectively.

Contributions: In summary, our main contributions are summarized as follows:

- We introduce a novel research problem, namely Generalized Unbiased Scene Graph Generation (G-USGG), which takes into account both predicate-level and concept-level imbalance, and develop a new metric (mCR@K) as a complement to mR, enabling evaluation of SGG models across concepts within predicates.
- We propose the Multi-Concept Learning (MCL) framework, which can be seamlessly integrated into both conventional and unbiased SGG methods, addressing both predicate-class and concept-class imbalance for G-USGG.
- Extensive experiments conduct on VG-SGG and OI-SGG datasets demonstrate the effectiveness and flexibility of our MCL, showcasing its capability of enhancing models' compositional generalizability and unbiased relation recognition capability.

II. Related Works

Unbiased Scene Graph Generation. Unbiased Scene Graph Generation (USGG) [25] requires SGG models to generate fine-grained predicates in the presence of long-tailed class distributions. To achieve that, TDE [25] leverages counterfactual causality to remove the modality bias from model's biased predictions. CogTree [15] constructs a hierarchical cognitive tree of predicates, which enhances the model's performance on easily confused predicates. BGNN [17] presents a confidence-aware bipartite graph neural network with an adaptive message propagation mechanism to mitigate the imbalanced data distribution problem. Additionally, NICE [26] introduces a strategy that not only detects noisy samples but also refines the predicate labels, resulting in an overall improvement on model's performance. RTPB [27] is designed to improve model's capability of detecting less frequent relationships by utilizing prior bias derived from the data distribution. Despite alleviating the predicate-level biased problem to some extent, all of them neglect the concept-level imbalance within predicates. Therefore, we focus on achieving both predicate-

level USGG and concept-level balanced recognition across concepts, addressing the G-USGG problem.

Prototypical Learning. The prototypical learning has been widely adopted in various domains, including Image Segmentation [23], [34], Few-shot Learning [34]–[36], and Source-free Domain Adaptation [37], [38]. Okazawa et al. [34] proposes an inter-class prototypical relation module to enhance the distinctiveness between different classes. Moreover, BMD [37] introduces an intra-class multi-center clustering strategy to achieve robust and representative prototype generation. [35] devises a decomposed prototype space that effectively captures intrinsic visual features of subjects and objects for few-shot relation recognition. Additionally, the ProCA [38] identifies target label prototypes and enforces the model to retain previous knowledge, alleviating domain discrepancies and catastrophic forgetting issues. However, these prototype-based methods neglect the fact that each class exhibits varying levels of complexity. Consequently, uniformly setting the same number of prototypes for all classes may result in issues of prototype redundancy and collapse. To the end, we propose to set different amounts of prototypes for different classes.

Memory-based Learning. Memory-based learning [39]–[43] has demonstrated its effectiveness in capturing diverse representations over extended periods. HML [44] is designed to mimic human hierarchical memory-based learning behavior, whereas models learn fine-grained predicates while benefiting from the memory of coarse ones. Moreover, PMN [41] uses memory banks to store useful prototypes from past frames for mask prediction in future frames. Lyu et al. [43] proposes an attentive memory network to effectively exploit the historical dialog information for reliable question answering. Besides, Zhu et al. [40] transfer knowledge from head to tail classes by storing biased representations, thereby addressing the imbalance issue across classes. In [42], memory banks are leveraged to store high-quality features from labeled data, enhancing the class separability. However, the aforementioned methods overlook two crucial aspects: 1) the importance of representative samples, and 2) the potential imbalance in memory-based representations. To the end, we devise balanced memory banks, which have fixed sizes and required carefully select representative samples for memory updating.

III. Methodology

A. Preliminary

Given input images $\boldsymbol{\mathcal{X}} = \{\boldsymbol{x_i}\}_{i=1}^{N}$, the task of SGG targets at generating the directed graph $\boldsymbol{\mathcal{G}} = \{\boldsymbol{\mathcal{V}}, \boldsymbol{\mathcal{E}}\}$, where $\boldsymbol{\mathcal{V}}$ is a set of entity nodes and $\boldsymbol{\mathcal{E}}$ is a set of relation edges. In scene graphs $\boldsymbol{\mathcal{G}}$, each entity node $\boldsymbol{\mathcal{V}}$ consists of bounding box coordinates $\mathbf{B} = \{\boldsymbol{b_i}\}_{i=1}^{N}$ and class labels $\mathbf{L} = \{\boldsymbol{l_i}\}_{i=1}^{N}$. Moreover, each edge $\boldsymbol{\mathcal{E}}$ connects two entity nodes (i.e., subjects and objects) and encodes the relationship between them, i.e., $\mathbf{P} = \{\boldsymbol{p_i}\} \in \mathbb{R}^{N \times P}$, where P denotes the amounts of predicate classes in SGG dataset. Generally, SGG models adopt a two-stage detection process. In the first stage, the Faster R-CNN is used to extract entity features $\mathbf{V} = \{\boldsymbol{v_i}\} \in \mathbb{R}^{N \times 4096}$, their word embedding (i.e., GloVe [45]) $\mathbf{Z} = \{\boldsymbol{z_i}\} \in \mathbb{R}^{N \times 300}$, and bounding boxes features $\mathbf{B}' = \{\boldsymbol{b'_i}\} \in \mathbb{R}^{N \times 128}$ within each image. Then, these features are concatenated and refined in the second stage by a contextual learning module $\mathbf{F}$ (e.g., Transformer in [27], Bi-LSTM in [29], and GCN in [46]), resulting in the conventional relation features $\mathbf{U} = \{\boldsymbol{u_i}\} \in \mathbb{R}^{N \times 4096}$. Finally, the relation features between subjects $\mathbf{S} = \{\boldsymbol{s_i}\}_{i=1}^{N}$ and objects $\mathbf{O} = \{\boldsymbol{o_i}\}_{i=1}^{N}$ are matched to their nearest predicate prototypes in the prototypical space for relation recognition.

B. Overview

To solve the G-USGG issue, we develop the MCL learning framework, illustrated in Fig. 2, encompassing following steps:

Step-1: In *Concept-Prototype Construction (CPC)*, we first conduct quantitative analysis of semantic scales across predicates and thereby quantify them into different amounts of concept-prototypes within a single predicate class, shown in Fig. 3. Then, these concept-prototypes are initialized in the prototypical space by uniformly sampling from a hyper-sphere with the radius as $r = 1$.

Step-2: Following the two-stage procedure (Sec. III-A), we first get the conventional relation features $\mathbf{U} = \{\boldsymbol{u_i}\}$ encoded from any context module within SGG models [20], [29], [33], [47], [48]. Then, the relation features (i.e., Eq. 5) are fused with the prototypical representations derived from the *Balanced Prototypical Memory (BPM)* (saving representative samples for each concept, Alg. 1), resulting in balanced relation representation $\mathbf{U}' = \{\boldsymbol{u'_i}\}$.

Step-3: With the balanced relation representations $\mathbf{U}' = \{\boldsymbol{u'_i}\}_{i=1}^{N}$, we perform the *Concept-guided Predicate Matching* for relation recognition. In this process, relation features are firstly matched to their corresponding concept-prototypes $\boldsymbol{\mathcal{C}} = \{\boldsymbol{c_k}\}_{k=1}^{K} \in \mathbb{R}^{K*4096}$ (i.e., Eq. 7), and then transferred to the corresponding predicate class for classification (i.e., Eq. 8, and Eq. 9). Finally, the *Concept Regularization (CR)* (including *Entity Dispersion Loss* $\mathcal{L}_e$ (i.e., Eq. 10), *Predicate Dispersion Loss* $\mathcal{L}_p$ (i.e., Eq. 12) and *Concept Dispersion Loss* $\mathcal{L}_c$ (i.e., Eq. 13)) is proposed to assist SGG models in effectively learning the *Concept-guided Predicate Matching*, by mitigating the predicate-level semantic overlap ($\mathcal{L}_e$, $\mathcal{L}_p$), and meanwhile enhancing the discriminability among concept-prototypes ($\mathcal{L}_c$). This collaborative effort, along with the BPM, helps SGG models learn concepts in a balanced manner.

C. Concept-Prototype Construction

To capture the variation of concepts and represent diverse concepts within a single class, we propose a technique called Concept-Prototype Construction (CPC). In CPC, we first assess the semantic scales of predicates based on their divergent distribution across contexts. Subsequently, we quantize the semantic scales into different amounts of concept-prototypes and initialize them in the prototypical space, representing various concepts within the same predicate.

Quantification of Semantic Scales. Each predicate class exhibits different semantic scales, which reveals their varying semantic diversity (i.e., different amounts of concepts). Furthermore, these semantic scales can be measured by the volume of predicates' involved contexts in SGG datasets (i.e.,

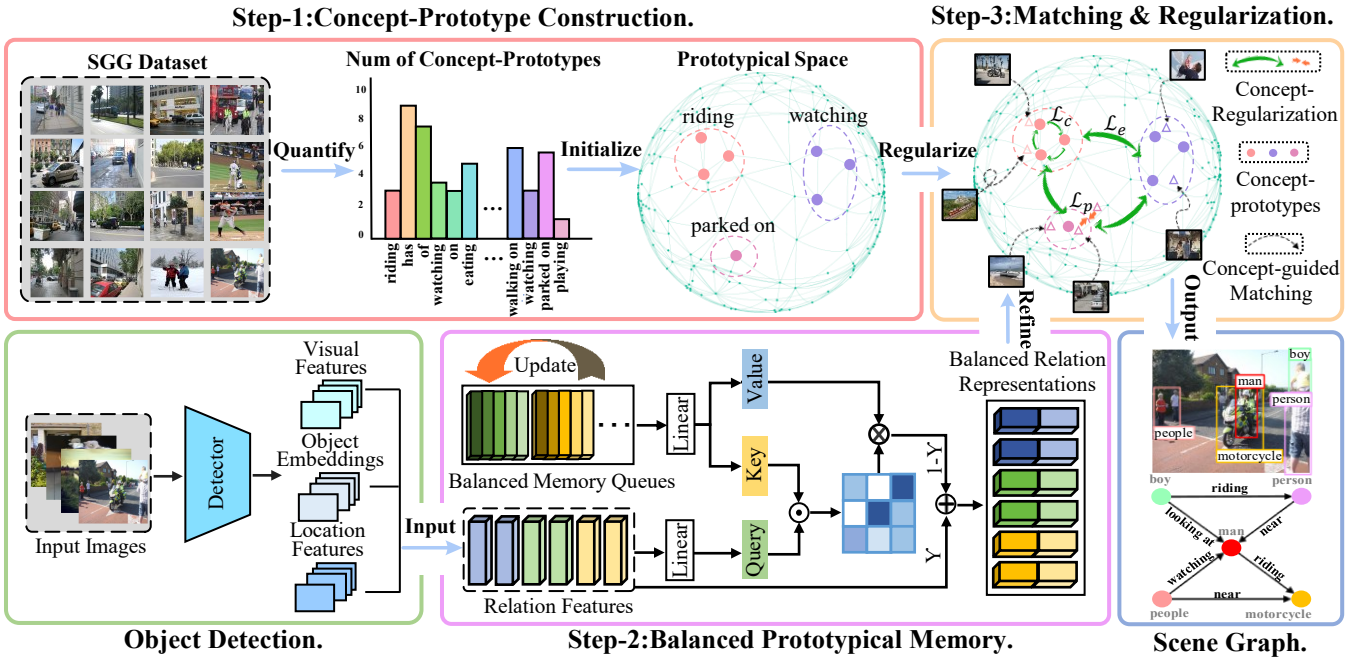

Fig. 2. **The Overview of our Multi-Concept Learning (MCL) framework**. It contains three parts: Concept-Prototype Construction (CPC), Balanced Prototypical Memory (BPM), and Concept Regularization (CR). The CPC assesses the semantic scales of each predicate from the SGG dataset and then quantifies the semantic scales into different amounts of concept-prototypes within the same predicate. Subsequently, BPM produces the balanced relation representations across different concepts within predicates, enabling the SGG model to equally attend to all concepts. Finally, the CR alleviates the predicate-level semantic overlap while enhancing the discriminability among concept-prototypes.

the range of all possible subject-object combinations). For instance, the semantic scale of "parked on" is typically lower than that of "on" due to the consistent association of "parked on" with subjects such as "bike/ car/ motorcycle/ truck" and objects such as "street/ sidewalk".

Practically, in CPC, we assess the semantic scales of predicate classes by measuring volumes of their decomposed subspace (i.e., subject-object pairs). To achieve that, we obtain word embeddings, i.e., $\boldsymbol{\mathcal{Z}} = \{\boldsymbol{z_i}\} \in \mathbb{R}^{K\times 600}$, of all possible contexts involved with the same predicate class from samples $\boldsymbol{\mathcal{X}} = \{\boldsymbol{x_i}\}_{i=1}^{N}$ in the SGG dataset. Then, these word embeddings are decomposed into subject embeddings $\boldsymbol{\mathcal{Z}_s} = \{\boldsymbol{z_i^s}\} \in \mathbb{R}^{K\times 300}$ and object embeddings $\boldsymbol{\mathcal{Z}_o} = \{\boldsymbol{z_i^o}\} \in \mathbb{R}^{K\times 300}$. Furthermore, the volumes of semantic scales $Vol(\boldsymbol{Z})$ are derived by calculating the covariance matrix between $\boldsymbol{\mathcal{Z}_s}$ and $\boldsymbol{\mathcal{Z}_o}$:

$$Vol(\boldsymbol{Z}) = \frac{1}{2}\log_2 \det(\boldsymbol{I} + (\boldsymbol{Z_s} - \overline{\boldsymbol{Z}}_{\boldsymbol{s}})(\boldsymbol{Z_o} - \overline{\boldsymbol{Z}}_{\boldsymbol{o}})^T), \quad (1)$$

where $\overline{\boldsymbol{Z}}_{\boldsymbol{s}}$ and $\overline{\boldsymbol{Z}}_{\boldsymbol{o}}$ are the mean values of $\boldsymbol{Z_s}$ and $\boldsymbol{Z_o}$, respectively. Intuitively, the larger the $Vol(\boldsymbol{Z})$, the more concepts the predicate class has. Next, we quantify the semantic scales $Vol(\boldsymbol{Z})$ into different amounts of concept-prototypes $\boldsymbol{M} = \{m_p\} \in \mathbb{R}^P$, as depicted in Fig 3:

$$m_p = f(Vol(\boldsymbol{Z})) = W_c(Vol(\boldsymbol{Z})) + b_c, \quad (2)$$

$$\mathrm{K} = \sum_{\mathrm{p}=1}^{\mathrm{P}} \mathrm{m_p}, \quad (3)$$

where K is the total amounts of prototypes across all predicates, and f is a predefined linear function with coefficient as W_c and bias as b_c.

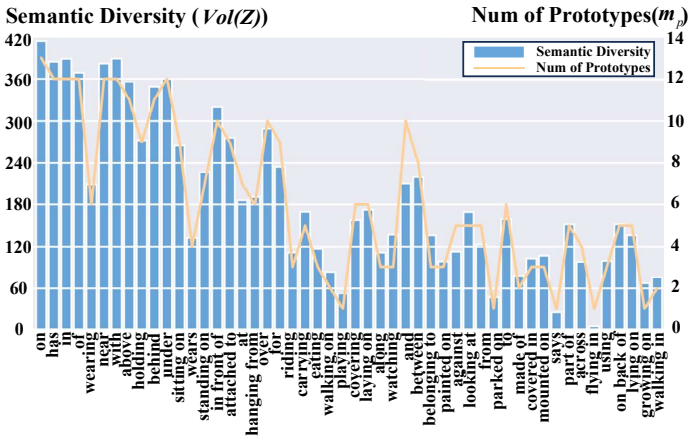

Fig. 3. **Quantitative analysis of semantic scales across predicate classes.** The predicates are sorted by their frequencies in VG-SGG.

Concept-Prototype Initialization. As stated in [49]–[52], a well-separated prototypical latent space may benefit the prototypical learning process from fully exploring different characteristics within the same class. To make concept-prototypes distinct in the prototypical space, we first initialize a hyper-sphere with the dimension as 4096 with the radius of 1, and then uniformly sample K points as concept-prototypes $\boldsymbol{\mathcal{C}} = \{\boldsymbol{c_k}\} \in \mathbb{R}^{K*4096}$ from the hyper-sphere. Then, we partition the K concept-prototypes into P predicate groups based on different amounts of concept-prototypes $\boldsymbol{M} = \{m_p\} \in \mathbb{R}^P$ within each predicate. This ensures that concept-prototypes belonging to the same class are close to each other in the prototypical space and far away from those belonging to

different classes.

D. Balanced Prototypical Memory

Due to the concept-level imbalance of G-USGG, relation features extracted from models $\mathbf{U} = \{\boldsymbol{u_i}\} \in \mathbb{R}^{N\times 4096}$ are dominated by common concepts, leaving rare/ uncommon concepts under-represented. It significantly degrades model's compositional generability across contexts within predicates. Therefore, we propose a memory-guided training strategy, namely Balanced Prototypical Memory (BPM), which saves/ derives concept-inherent prototypical representations $\boldsymbol{\Omega} = \{\boldsymbol{\omega_k}\}_{k=1}^{K}$ from the balanced memory, and thereby complicates them with biased representations generating balanced relation representations $\mathbf{U'} = \{\boldsymbol{u'_i}\} \in \mathbb{R}^{N\times 4096}$ across concepts.

Balanced Relation Representation Generation. In BMP, we first build a dictionary of memory queues $\mathbf{Q} = \{\boldsymbol{Q_k}\}_{k=1}^{K}$, which save samples belonging to different concepts k within predicates. Moreover, the prototypical representation $\boldsymbol{\Omega} = \{\boldsymbol{\omega_k}\}_{k=1}^{K}$ is derived by averaging instance representations saved in the queue $\boldsymbol{Q_k}$ for each concept k, which is the abstract of concept-prototypes $\boldsymbol{\mathcal{C}} = \{\boldsymbol{c_k}\}_{k=1}^{K}$. By ensuring that all queues are of the same fixed size $|\boldsymbol{Q_k}|$, prototypical representations become more balanced across concepts compared to the conventional relation features derived from SGG models. Practically, given the conventional relation features $\mathbf{U} = \{\boldsymbol{u_i}\}$, BPM first retrieves the most relevant prototypical representations of concept k (i.e., $\boldsymbol{\Omega} = \{\boldsymbol{\omega_k}\}_{k=1}^{K}$) from $\boldsymbol{Q_k}$, utilizing the Multi-head Self-Attention mechanism [48],

$$\begin{aligned} \boldsymbol{\omega_c} &= \mathrm{Concat}(\mathbf{head_1}, ..., \mathbf{head_h})\boldsymbol{W^O}, \\ \mathbf{head_i} &= \mathrm{Attention}(\boldsymbol{QW_i^Q}, \boldsymbol{KW_i^K}, \boldsymbol{VW_i^V}) \end{aligned} \tag{4}$$

where $\boldsymbol{W_i^Q}, \boldsymbol{W_i^K}, \boldsymbol{W_i^V}, \boldsymbol{W^O} \in \mathbb{R}^{4096\times 4096}$ are learnable parameters. Moreover, $\boldsymbol{K} = \boldsymbol{V} = \boldsymbol{\Omega}$ and $\boldsymbol{Q} = \boldsymbol{u_i}$. Then, the retrieved prototypical representations $\boldsymbol{\omega_c}$ are fused with relation features $\boldsymbol{u_i}$, resulting in balanced relation representations $\boldsymbol{u'_i}$,

$$\boldsymbol{u'_i} = \lambda \boldsymbol{u_i} + (1-\lambda)\boldsymbol{\omega_c}, \tag{5}$$

where λ is a hyper-parameter to make a trade-off between prototypical representations and conventional relation features.

Balanced Memory Updating. To make the prototypical representations of each concept more representative, we update the memory queues $\mathbf{Q} = \{\boldsymbol{Q_k}\}_{k=1}^{K}$ in BMP with high-confident and diverse samples from coming-batch $\boldsymbol{\mathcal{X}^t} = \{\boldsymbol{x_i^t}\}_{i=1}^{N}$. The intuitive explanation of the Balanced Memory Updating (BMU) regime with the Peruse-code is provided in Alg. 1. For each iteration, we first acquire model's predicted logits towards each concept as $\boldsymbol{\eta^c} = [\eta_1^c, \eta_2^c, ..., \eta_K^c]$ and perform the $Argmax$ function to find the index of matched concept k with highest logits η_k^c. Then, if η_k^c is larger than the confidence-threshold ξ, the incoming sample $\boldsymbol{x_i^t}$ together with its time step t would be saved into its corresponding queue $\boldsymbol{Q_k}$. Furthermore, to capture the variation within concepts, BPM stores samples with diverse contexts, generating more representative prototypical representations. In practice, the BPM saves samples whose word embeddings of contexts are diverse by calculating the hamming score $\mathbf{H(i)}$ between the incoming sample $\boldsymbol{x_i^t}$ and those saved in queue $\boldsymbol{Q_k}$,

$$\mathbf{H}(\mathbf{x_i^t}, \mathbf{Q_k}) = \frac{1}{|\boldsymbol{Q_k}|}\sum_{i=1}^{|\boldsymbol{Q_k}|} \mathbf{Z}_i \cdot \mathbf{Z}_t, \tag{6}$$

where $\mathbf{Z}_t$ represents word embeddings of contexts within the incoming sample $\boldsymbol{x_i^t}$, and $\mathbf{Z}_i$ refers to word embeddings of samples saved in queue $\boldsymbol{Q_k}$. If the hamming score $\mathbf{H}(\mathbf{x_i^t}, \mathbf{Q_k})$ is larger than the threshold θ, the incoming sample $\boldsymbol{x_i^t}$ together with its time step t would be saved into the corresponding queue $\boldsymbol{Q_k}$. Moreover, when the queue $\boldsymbol{Q_k}$ is full, the oldest sample $\boldsymbol{x_i^0}$ would be replaced with the incoming sample $\boldsymbol{x_i^t}$.

Algorithm 1 Balanced Memory Updating

Input: Memory queues $\mathbf{Q} = \{\boldsymbol{Q_k}\}_{k=1}^{K}$, the incoming samples $\mathcal{X} = \{\boldsymbol{x_i^t}\}_{i=1}^{N}$, the Ground Truth $\boldsymbol{\mathcal{Y}} = \{y_i\}_{i=1}^{N}$, the confidence threshold ξ, the diversity threshold θ, and model's predictive logits $\boldsymbol{\eta^c} = [\eta_1^c, \eta_2^c, ..., \eta_K^c]$.
Output: Updated memory queues $\mathbf{Q'} = \{\boldsymbol{Q'_k}\}_{k=1}^{K}$.

```
for i = 0 to N do
    if: Q_k is not full then
        //* Update memory with high-confident samples.*//
        if: Argmax(η^c) = y_i and η_i^c > ξ then
            Append sample x_i^t together with time step t to Q_k.
        end if:
    else
        //* Update memory queues with diverse samples.*//
        if: H(x_i^t, Q_k) > θ then
            Replace the oldest sample x_i^0 in Q_k with incoming sample x_i^t.
        end if:
    end if:
end for
```

E. Concept-guided Predicate Matching

After obtaining the balanced relation representation from BPM, we perform the Concept-guided Predicate Matching, whereas the balanced relation features $\mathbf{U'} = \{\boldsymbol{u'_i}\}_{i=1}^{N}$ of samples $\boldsymbol{\mathcal{X}} = \{\boldsymbol{x_i}\}_{i=1}^{N}$ are firstly matched to their corresponding concept-prototypes $\boldsymbol{\mathcal{C}} = \{\boldsymbol{c_k}\}_{k=1}^{K} \in \mathbb{R}^{K*4096}$ (i.e., Eq. 7) using concept-level matching scores $\boldsymbol{\eta^c}$. Then, these scores are accumulated as predicate-level scores $\boldsymbol{\eta^p}$ for relation recognition (i.e., Eq. 8, Eq. 9),

$$\boldsymbol{\eta^c} = \langle \boldsymbol{u'_i}, \boldsymbol{c_k} \rangle / \tau, \tag{7}$$

$$\boldsymbol{\eta^p} = \frac{1}{m_p}\sum\nolimits_{\boldsymbol{c_k}\in p} res_i^c, \tag{8}$$

$$res_i^p = \underset{i}{\mathrm{argmax}}(\{\boldsymbol{x_i}|\boldsymbol{\eta^p}\}), \tag{9}$$

where res_i^p and res_i^c indicate model's concept-level and predicate-level relation matching results. Moreover, m_p and τ are amounts of concept-prototypes within single predicate class and learnable temperature hyper-parameter, respectively.

F. Concept Regularization

To effectively learn the Concept-guided Predicate Matching for addressing the G-USGG problem, we introduce the Concept Regularization (CR), which aims to simultaneously ① **promote the discriminability of concept-prototypes within the same predicate class**, effectively dealing with the multi-prototype collapse problem [49]–[52], and ② **encourage the dispersion between predicates by considering both class-level prototypes and instance-level representations**, thereby reducing the semantic overlap [15], [18], [44], [53] between predicates.

To achieve ①, we propose both *Entity Dispersion Loss ($\mathcal{L}_e$)* and *Predicate Dispersion Loss ($\mathcal{L}_p$)*, which gently encourage instances and prototypes to move away from instances and prototypes belonging to different predicate classes. For every pair of relation features $\boldsymbol{u'_{p_i}}$ and $\boldsymbol{u'_{p_j}}$ from different classes, we enlarge their distance in model's latent space by imposing the constraint of $\mathcal{L}_e$,

$$\mathcal{L}_e(\boldsymbol{u'}_{p_i}, \boldsymbol{u'}_{p_j}) = -\log \frac{\exp(\boldsymbol{u'}_{p_i} \cdot \boldsymbol{u'}_{p_j})}{\sum_{\boldsymbol{u'}_p \in \boldsymbol{U'} \setminus \boldsymbol{u'}_{p_i}} \exp(\boldsymbol{u'}_{p_i} \cdot \boldsymbol{u'}_p)}. \tag{10}$$

The $\mathcal{L}_e$ only considers the instance-level distance, which may result in a lack of class-level distinctiveness in the prototypical space. To this end, we propose a *Predicate Dispersion Loss ($\mathcal{L}_p$)*, which encourages the class-level separation between groups of concept-prototypes belonging to different predicates. Practically, the holistic prototypical representation for a group of concept-prototypes $\boldsymbol{\mathcal{D}} = \{\boldsymbol{d_p}\}_{p=1}^{P} \in \mathbb{R}^{P \times 4096}$ is derived by averaging representations of concept-prototypes $\boldsymbol{\mathcal{C}} = \{\boldsymbol{c_k}\} \in \mathbb{R}^{K \times 4096}$ within the same class p,

$$\boldsymbol{d_p} = \frac{1}{m_p} \sum\nolimits_{\boldsymbol{c_k} \in p} \boldsymbol{c_k}. \tag{11}$$

Then, we increase the distance between a group of concept-prototypes $\boldsymbol{c^k_{p_i}}$ (belonging to predicate p_i) and the holistic prototypical representation $\boldsymbol{d_{p_j}}$ (belonging to predicate p_j) by imposing $\mathcal{L}_p$,

$$\begin{aligned} \mathcal{L}_p(\boldsymbol{c}^k_{p_i}, \boldsymbol{d}_{p_j}) &= -\log \frac{\exp(\boldsymbol{c}^k_{p_i} \cdot \boldsymbol{d}_{p_j})}{\sum_{\boldsymbol{d}_{p_j} \in \boldsymbol{D}} \exp(\boldsymbol{c}^k_{p_i} \cdot \boldsymbol{d}_{p_j})}, \\ \mathcal{L}_p(\boldsymbol{\mathcal{C}}, \boldsymbol{\mathcal{D}}) &= \sum_{p_j=1}^{P} \sum_{c=1}^{m_{p_i}} \mathcal{L}_p(\boldsymbol{c}^k_{p_i}, \boldsymbol{d}_{p_j}). \end{aligned} \tag{12}$$

To achieve ②: we propose a *Concept Dispersion Loss ($\mathcal{L}_c$)* that ensures the discriminability among concept-prototypes within the same predicate. In the absence of this loss, models tend to align instances from the same predicate to a single concept-prototype, neglecting rare/ uncommon concepts (depicted in Fig. 6). This leads an imbalanced learning process across concepts within the same predicate. To address this, the $\mathcal{L}_c$ is proposed to enlarge distances between concept-prototypes $\boldsymbol{c_i}$ and $\boldsymbol{c_j}$ within the same class,

$$\mathcal{L}_p(\boldsymbol{c}_i, \boldsymbol{c}_j) = -\log \frac{\exp(\boldsymbol{c}_i \cdot \boldsymbol{c}_j)}{\sum_{\boldsymbol{c}_k \in \boldsymbol{C} \setminus \boldsymbol{c}_i} \exp(\boldsymbol{c}_i \cdot \boldsymbol{c}_k)}. \tag{13}$$

G. Training

With the predicate-level matching results res_i^p derived from the Concept-guided Predicate Matching, we further apply the $\mathcal{L}_{CE}$ to encourage the relation representation $\boldsymbol{u'_i}$ to be close to its corresponding concept-prototype in the prototypical space,

$$\mathcal{L}_{CE}(\boldsymbol{\eta^p}) = -\textstyle\sum_{i=1}^{P} w_i y_i \log(\eta_i^p) \ , \tag{14}$$

where w_i is the class-specific weight widely used in USGG methods [14], [15], [19], [25]–[27], [54]. Moreover, during the training stage, the final loss function $\mathcal{L}$ for our MCL is expressed as:

$$\mathcal{L} = \mathcal{L}_{CE} + \mathcal{L}_e + \mathcal{L}_p + \mathcal{L}_c. \tag{15}$$

IV. Experiments

A. Datasets

Following previous works [17], [19]–[21], [55], we conduct experiments on both the Visual Genome (VG-SGG) [56] and the Open Image (OI-SGG) [57] datasets. The VG-SGG contains 108k images with 150 entity categories and 50 predicate categories. Furthermore, we divide 70% of the data as the training set and 30% as the test set to validate the effectiveness of the model. Additionally, we select $5,000$ images from the training set as the validation set. Moreover, the OI-SGG has 301 entity classes and 31 predicate classes with $85k$ images and $472k$ relations, following the 70%-30% data split.

B. Evaluation Metrics

Based on the prior works [17], [47], we evaluate our methods on three sub-tasks of SGG, including **PredCls** (Predicate Classification), **SGCls** (Scene Graph Classification), and **SGDet** (Scene Graph Detection). Following recent works [18], [47], [54], [58], [59], we take the Recall (**R@K**), mean Recall (**mR@K**), and F-score@K (**F@K**) as the evaluation metrics. Moreover, we evaluate SGG methods utilizing the Few-shot Recall@K (**Fs-R@K**) and Zero-shot Recall@K (**Zs-R@K**) to demonstrate their effectiveness in handling rare/ unseen triplets. Finally, to comprehensively evaluate model's compositional generability (i.e., model's performance across concepts within the same predicate), we introduce the mean Context Recall (**mCR@K**), which calculates the recall of each predicate under all possible contexts (i.e., subject-object combinations) independently, and then averages the results across every predicate. To clarify, we provide the Peruse-code of calculation of mCR@K in the Alg. 2.

C. Implementation Details

Detector. In line with most of the mainstream SGG models [14], [27], [29], [47], we utilize the pre-trained Faster R-CNN model trained by [58], [60] to detect entities in images.

Scene Graph Generation. All SGG models are trained with Cross-Entropy Loss and SGD optimizer with an initial learning rate of 0.001, batch-size of 8, and at most 60k iterations.

Multiple Concept Learning. We merge our Multiple Concept Learning (MCL) into several benchmark models in the Model

TABLE I
COMPARISON BETWEEN EXISTING METHODS AND OUR MCL UNDER THREE SUB-TASKS OF R@K, MR@K, AND F@K(%) ON THE VG-SGG DATASET.

Model	Method	PredCls			SGCls			SGDet		
		R@50/100	mR@50/100	F@50/100	R@50/100	mR@50/100	F@50/100	R@50/100	mR@50/100	F@50/100
Motifs [29]	- Baseline$_{CVPR'18}$	**59.6 / 63.9**	12.8 / 15.5	21.1 / 24.9	**36.5 / 38.5**	7.7 / 8.8	12.7 / 14.3	**26.9 / 30.5**	5.6 / 6.7	9.2 / 10.9
	+ GCA [32]$_{ICCV'21}$	58.2 / 60.4	17.8 / 18.3	27.3 / 28.1	34.2 / 35.3	11.2 / 12.6	22.7 / 23.9	26.0 / 29.8	9.0 / 10.2	17.5 / 20.0
	+ PPDL [61]$_{CVPR'22}$	47.2 / 47.6	32.2 / 33.3	38.3 / 39.2	28.4 / 29.3	17.5 / 18.2	21.6 / 22.4	21.2 / 23.9	11.4 / 13.5	14.8 / 17.2
	+ Inf [24]$_{CVPR'23}$	51.5 / 55.0	24.7 / 30.7	33.4 / 39.4	32.2 / 33.8	14.5 / 17.4	23.1 / 24.1	23.9 / 27.1	9.4 / 11.7	13.4 / 16.3
	+ NICE [26]$_{CVPR'22}$	55.1 / 57.2	29.9 / 32.3	38.7 / 41.2	33.1 / 34.0	16.6 / 17.9	22.1 / 23.4	27.8 / 31.8	12.2 / 14.4	16.9 / 19.8
	+ HML [44]$_{ECCV'22}$	47.1 / 49.1	36.3 / 38.7	41.0 / 43.3	26.1 / 27.4	20.8 / 22.1	23.1 / 24.4	17.6 / 21.1	14.6 / 17.3	15.9 / 19.0
	+ Debiasing [1]$_{CVPR'19}$	53.2 / 55.5	33.7 / 36.1	41.3 / 43.7	32.1 / 33.4	17.7 / 19.1	22.8 / 24.3	25.1/ 28.2	13.3 / 15.4	17.4 / 19.9
	+ IETrans [14]$_{ECCV'22}$	50.0 / 52.1	35.1 / 37.8	41.2 / 43.8	28.0 / 28.9	19.2 / 20.4	22.7 / 23.9	21.5 / 29.8	13.6 / 15.3	16.6 / 20.2
	+ MCL	59.4 / 62.1	**39.6 / 41.9**	**47.5 / 50.0**	34.5 / 35.8	**23.7 / 25.1**	**28.1 / 29.5**	26.2 / 30.4	**15.3 / 17.8**	**19.3 / 22.5**
VCTree [47]	- Baseline$_{CVPR'19}$	**65.9 / 67.5**	17.1 / 18.4	27.2 / 28.9	**40.5 / 41.4**	10.8 / 11.5	17.0 / 18.0	**32.0 / 36.2**	7.2 / 8.4	11.7 / 13.6
	+ PPDL [61]$_{CVPR'22}$	47.6 / 48.0	33.3 / 33.8	39.1 / 39.6	32.1 / 33.0	21.8 / 22.4	25.9 / 26.8	20.1 / 22.9	11.3 / 13.3	14.4 / 16.8
	+ BPL-SA [16]$_{ICCV'21}$	50.0 / 51.8	30.6 / 32.6	37.9 / 40.0	34.0 / 35.0	20.1 / 21.2	25.2 / 26.4	21.7 / 25.5	13.5 / 15.7	16.6 / 19.4
	+ GCL [13]$_{CVPR'22}$	40.7 / 42.7	37.1 / 39.1	38.8 / 40.8	27.7 / 28.7	22.5 / 23.5	25.8 / 25.9	17.4 / 20.7	15.2 / 17.5	16.2 / 18.9
	+ IETrans [14]$_{ECCV'22}$	53.0 / 55.0	30.3 / 33.9	38.6 / 41.9	32.9 / 33.8	16.5 / 18.1	22.0 / 23.6	25.4 / 29.3	11.5 / 14.0	15.8 / 18.9
	+ MCL	59.5 / 61.9	**39.0 / 41.6**	**47.1 / 49.8**	36.0 / 37.3	**23.1 / 24.5**	**28.1 / 29.6**	26.1 / 30.1	**15.2 / 17.7**	**19.2 / 22.3**
Transformer [48]	- Baseline $_{NIPS'17}$	**65.7 / 67.7**	16.0 / 17.5	25.7 / 27.8	**40.1 / 41.0**	9.6 / 10.2	15.4 / 16.3	**32.9 / 37.6**	7.3 / 8.8	11.9 / 14.2
	+ RTPB [27]$_{AAAI'22}$	50.6 / 52.6	26.7 / 28.4	34.9 / 36.8	27.0 / 28.0	17.4 / 18.2	21.1 / 22.0	19.1 / 22.9	14.1 / 16.1	16.2 / 18.9
	+ BPL-SA [16]$_{ICCV'21}$	48.4 / 50.2	31.9 / 34.2	38.4 / 40.6	29.8 / 30.6	18.5 / 19.4	22.8 / 23.7	25.5 / 29.9	13.5 / 15.7	17.6 / 20.5
	+ IETrans [14]$_{ECCV'22}$	51.8 / 53.8	30.8 / 34.7	38.6 / 42.2	32.6 / 33.5	17.4 / 19.1	22.7 / 24.3	25.5 / 29.6	12.5 / 15.0	16.8 / 19.9
	+ MCL	58.5 / 60.9	**39.2 / 41.6**	**46.9 / 49.4**	35.9 / 37.2	**23.4 / 25.0**	**28.1 / 29.6**	27.1 / 31.3	**14.8 / 17.2**	**19.2 / 22.2**
TDE [25]	- Baseline$_{CVPR'20}$	45.9 / 51.2	24.8 / 28.7	32.2 / 36.8	26.3 / 28.8	13.2 / 15.1	17.5 / 19.8	16.3 / 19.5	8.7 / 10.5	11.3 / 13.6
	+ DeC [31]$_{TIP'23}$	49.5 / 51.3	25.1 / 28.9	33.3 / 36.9	25.3 / 28.7	14.2 / 16.1	18.2 / 20.6	21.4 / 25.2	12.0 / 13.6	15.3 / 17.6
	+ Inf [24]$_{CVPR'23}$	42.4 / 46.8	28.6 / 35.7	34.1 / 40.5	24.1 / 26.3	15.9 / 18.9	19.1 / 21.9	15.1 / 18.0	9.6 / 11.9	11.7 / 14.3
	+ MCL	**55.5 / 57.7**	**35.3 / 37.3**	**43.1 / 45.3**	**34.4 / 35.4**	**19.5 / 20.5**	**24.9 / 26.0**	**26.4 / 30.5**	**14.9 / 17.2**	**19.0 / 22.0**
PENET [20]	- Baseline$_{CVPR'23}$	58.7 / 61.5	38.4 / 39.9	46.4 / 48.3	35.8 / 37.0	22.8 / 23.1	27.8 / 28.4	26.9 / 31.3	14.5 / 17.0	18.8 / 22.0
	+ MCL	**59.3 / 61.8**	**40.2 / 42.4**	**47.9 / 50.3**	**36.2 / 37.5**	**23.3 / 24.8**	**28.4 / 29.9**	**27.3 / 31.7**	**14.9 / 17.3**	**19.3 / 22.4**
SQUAT [33]	- Baseline$_{CVPR'23}$	55.7 / 57.9	30.9 / 33.4	39.7 / 42.3	33.1 / 34.4	17.5 / 18.8	22.8 / 24.3	24.5 / 28.9	14.1 / 16.5	19.7 / 20.9
	+ MCL	**59.5 / 61.9**	**37.4 / 39.7**	**45.9 / 48.4**	**35.9 / 37.1**	**22.9 / 24.4**	**28.0 / 29.4**	**27.7 / 31.8**	**14.7 / 16.9**	**19.2 / 22.1**

Zoo. Moreover, based on the quantitative analysis of semantic scales, there are 307 prototypes in total for CPC. Regarding the memory queues, the memory size M is 64, the confidence threshold ξ is 0.9, and the diversity threshold θ is 0.5. Regarding the BPM, we set the value of λ to 0.95, which is one of the optimal value that leads to better performance.

Algorithm 2 Mean Context Recall (**mCR@K**)

Input: Recall@K I_{s_i,p_v,o_j} of predicate p under each possible context (s_i, o_j), the number of entity class N, the amounts of predicate class P.
Output: Mean Context Recall@K (**mCR@K**) ϕ^K.

```
Create a Set φ^K = {φ^K_{p_v}} ∈ R^P.
//* Traverse P predicate classes. *//
for p = 1 to P do
    //* Traverse N * N subject-object combinations.*//
    for i = 1, j = 1 to N do
        //* Accumulate Recall@K I_{s_i,p_v,o_j} of predicate p
        under all possible contexts (s_i, o_j). *//
        φ^K_{p_v} ← φ^K_{p_v} + I_{s_i,p_v,o_j}
    end for
    //* Average the Context Recall across predicates. *//
    φ^K ← φ^K + φ^K_{p_v}/(N * N)
end for
φ^K ← φ_{p_k}/P
```

D. Compare with State-of-the-art

To evaluate the capability of our methods in scene graph generation, we conduct comparisons with state-of-the-art methods on two SGG datasets, namely VG-SGG and OI-SGG.

TABLE II
COMPARISON WITH STATE-OF-THE-ART METHODS ON OPENIMAGES V6 UNDER SGDET TASK. WE ADOPT THE SAME EVALUATION METRICS AS [17].

Model	*SGDet*			
	R@50	wmAP$_{rel}$	wmAP$_{phr}$	score$_{wtd}$
Motifs [29]$_{CVPR'18}$	71.6	29.9	31.6	38.9
TDE [25]$_{CVPR'20}$	69.3	30.7	32.8	39.3
VCTree [47]$_{CVPR'19}$	74.1	34.2	33.1	40.2
RelDn [62]$_{CVPR'19}$	73.1	32.2	33.4	40.8
GPS-Net [62]$_{CVPR'20}$	74.8	32.9	34.0	41.7
GR-CNN [46]$_{ECCV'18}$	74.5	33.2	34.2	41.8
RU-Net [55]$_{CVPR'22}$	74.1	33.5	34.2	42.1
Dbiased-P [63]$_{TMM'22}$	74.6	34.3	34.4	42.3
PCL [64]$_{TIP'22}$	74.8	34.7	35.0	42.8
RelTR [65]$_{TPAMI'22}$	71.7	34.2	37.5	43.0
HL-Net [66]$_{CVPR'22}$	76.5	35.1	34.7	43.2
BGNN [17]$_{CVPR'21}$	75.0	35.4	34.9	43.5
SQUAT [33]$_{CVPR'23}$	75.8	34.9	35.9	43.5
Debiasing [1]$_{CVPR'19}$	75.1	36.0	37.1	44.3
PE-Net [20]$_{CVPR'23}$	**76.5**	36.6	37.4	44.9
MCL	76.0	**37.2**	**38.2**	**45.4**

Quantitative analysis on VG-SGG. We compare our MCL with state-of-the-art SGG models via merging it into several SGG benchmark models, namely Motifs [29], VCTree [47], Transformer [48], SQUAT [33], and PENET [20]. Quantitative results compared with state-of-the-art plug-and-play methods on the VG-SGG dataset are shown in Tab. I. We observe that our MCL consistently improves the performance on several SGG benchmark models. For instance, our MCL uniformly improves the performance of conventional SGG models (i.e., PENET (MCL), SQUAT (MCL), Motifs (MCL), Transformer (MCL), and VCTree (MCL)), reaching new state-of-the-art on VG-SGG dataset (e.g., for Motifs, 50.0%, 29.5% and 22.5% on F@100 across three sub-tasks), which confirms that our

MCL is orthogonal to the existing SGG methods for improving their capability of relation recognition.

Quantitative analysis on OI-SGG. To evaluate the effectiveness of our MCL across different data distributions, we conduct experiments on the OI-SGG dataset. The results obtained from the OI-SGG dataset are summarized in Tab. II. Similar to the performance achieved on the VG-SGG dataset, our MCL also reaches a new state-of-the-art on the OI-SGG dataset. Specifically, MCL significantly outperforms the state-of-the art method, i.e., PE-Net [20], on wmAP_{rel}, wmAP_{phr}, with improvements of 0.6%, 1.2%, resulting in a new state-of-the art of $\text{score}_{\text{wtd}}$=$45.4\%$ on the OI-SGG dataset. The possible reason is that our method captures the variation among different concepts within a single predicate class which allows SGG models to effectively predict predicates across different concepts, boosting their capability on relation recognition.

E. Generalized Unbiased Relation Recognition of MCL

In this section, we seek to answer the following questions:
Q1. Can our MCL achieve the predicate-level unbiased relation recognition in the presence of long-tailed predicates?
Q2. Can our MCL alleviate the concept-level imbalanced prediction issue of existing SGG models across rare/ uncommon/ common concepts?

Predicate-level Unbiased Relation Recognition. i) *Qualitative Analysis.* For an intuitive illustration of MCL's unbiased relation recognition, we compare R@100 results on each predicate between Motifs w/ MCL and Motifs w/o MCL, in Fig. 4. We observe that our MCL significantly improves the performance across almost all the predicates, (e.g., "walking in", "growing on", and "painted on"). The possible reason is that CR reduces the predicate-level overlap by enforcing larger distances between concepts with similar semantics but belonging to different predicate classes. By doing so, models can better differentiate between predicates and avoid potential confusion between similar concepts from different classes.
ii) *Quantitative Analysis.* We provide quantitative analysis to assess the effectiveness of MCL on enhancing the ability of unbiased relation recognition. The experiments are conducted on several SGG benchmark models (i.e., Motif, Transformer, VCTree, TDE, PENET and SQUAT) under the VG-SGG dataset, and the results for mR@K, R@K, and F@K metrics are reported in Tab. I. We find that our MCL pushes the performance of these SGG methods to a new level, surpassing SOTA USGG methods. For instance, our Motifs-MCL outperforms Motifs-IETrans 4.1%, 4.7% and 2.5% at mR@100 under the PredCls/ SGCls/ SGDet tasks. The experimental results provide strong evidence in support of our hypothesis that our method can enhance SGG models' predicate-level unbiased relation prediction capability in the presence of long-tail distributed predicates.

Concept-level Balanced Relation Recognition. So far, we can see that our MCL can enhance model's capability of unbiased relation recognition. Furthermore, it is essential to figure our whether MCL can also alleviate the concept-level imbalanced prediction issue of existing SGG models. To demonstrate that, we conduct experiments on several SGG benchmark models providing both qualitative (Fig. 5) and quantitative (Tab. III, Tab. IV) analysis.
i) *Qualitative Analysis.* For a comprehensive qualitative analysis, we visualize prediction results of Motifs w/ MCL and Motifs w/ Debiasing [1] on "holding" and "riding" across contexts in Fig 5. For "holding" (shown in Fig. 5(a)), the Motifs w/ Debiasing exhibits the extremely imbalanced performance across contexts (indicated by the **green** area). In contrast, the Motifs w/ MCL demonstrates balanced predictions across cocnepts. For instance, Motifs w/ MCL achieves balanced recognition results across most of the s/ o pairs from "hand-paper" to "man-child" (indicated by the red area). It highlights MCL's capability on dealing with the concept-level imbalanced prediction issue, ensuring balanced relation recognition across uncommon concepts within rare contexts.
ii) *Quantitative Analysis.* For the quantitative analysis, we compare our MCL with current SGG methods on VG-SGG with respect to Few-shot Recall/ mean Context Recall (Tab. III), and Zero-shot Recall metrics (Tab. IV), respectively. From Tab. III, we observe that our MCL consistently outperforms the other SGG debasing methods (i.e, FGPL [19], EBM [67], and Debiasing [1]) on all baselines (i.e., Motifs, VCTree, SQUAT, and PENET) at both Fs-R@100 and mCR@100 metrics. For instance, our Motifs+MCL outperforms Motifs+FGPL with 5.8% on mCR@100, and 1.6%, 2.5%, 1.8%, and 3.8% at Fs-R@100 on 1-5 shots, 6-10 shots, 11-20 shots, 21-30 shots. Additionally, in comparison with existing SGG methods on unseen triples (Tab. IV), we figure out that our MCL method reaches the best performance at Zs-R@50 and Zs-R@100 across three sub-tasks, reaching 22.3%, 6.8%, 4.1% at Zs-R@100 on all three sub-tasks. The above experiments demonstrate that our MCL effectively assists SGG models in capturing and learning diverse concepts in a balanced manner. The effectiveness can be attributed to the collaborative integration of Concept Regularization (CR) and Balanced Prototype Memory (BPM) in our method, which work together to enhance models' compositional generability across various contexts, encompassing both common, uncommon, and rare concepts.

TABLE III
COMPARISON WITH SGG METHODS AT FEW-SHOT RECALL (FS-R@100) AND MCR@100 UNDER THREE SUB-TASKS ON THE VG-SGG DATASET.

Model	Fs-R@100				mCR@100
	1-5 shots	6-10 shots	11-20 shots	21-30 shots	
Motifs+Debiasing	29.1 (-1.8)	35.6 (-0.9)	37.7 (-0.9)	42.6 (-2.8)	20.1 (-7.7)
Motifs+FGPL	29.3 (-1.6)	34.0 (-2.5)	36.8 (-1.8)	41.6 (-3.8)	22.1 (-5.8)
Motifs+MCL	**30.9**	**36.5**	**38.6**	**45.4**	**27.8**
VCTree+EBM	16.9 (-14.6)	25.2 (-11.8)	30.1 (-10.6)	32.6 (-13.9)	18.9 (-8.1)
VCTree+Debiasing	28.9 (-2.6)	32.5 (-4.5)	31.7 (-9.0)	39.8 (-6.7)	19.7 (-7.3)
VCTree+MCL	**31.5**	**37.0**	**40.7**	**46.5**	**27.0**
SQUAT+Debiasing	28.7 (-3.5)	32.0 (-4.8)	33.3 (-6.2)	40.0 (-5.3)	23.6 (-2.2)
SQUAT+MCL	**32.2**	**36.8**	**39.5**	**45.3**	**25.8**
PENET+Debiasing	22.6 (-10.0)	32.6 (-5.0)	33.1 (-6.1)	40.0 (-5.4)	25.3 (-1.5)
PENET+MCL	**32.6**	**37.6**	**39.2**	**45.4**	**26.8**

F. Ablation Study

In this section, we conduct an ablative analysis to examine the impact of MCL's components (i.e., CPC, BPM, and CR (including $\mathcal{L}_e, \mathcal{L}_p, \mathcal{L}_c$)) (Tab. V), and investigate the effects of

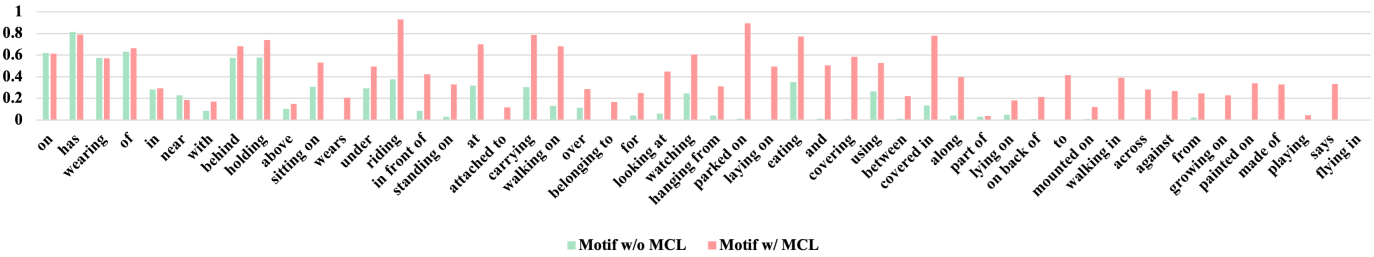

Fig. 4. **R@100 for all predicates of VG-SGG under the PredCls task between Motifs w/o MCL and Motifs w/ MCL.** The predicates are sorted by their frequencies in VG-SGG. Motifs w/ MCL achieves superior unbiased relation recognition performance in comparison with Motifs w/o MCL.

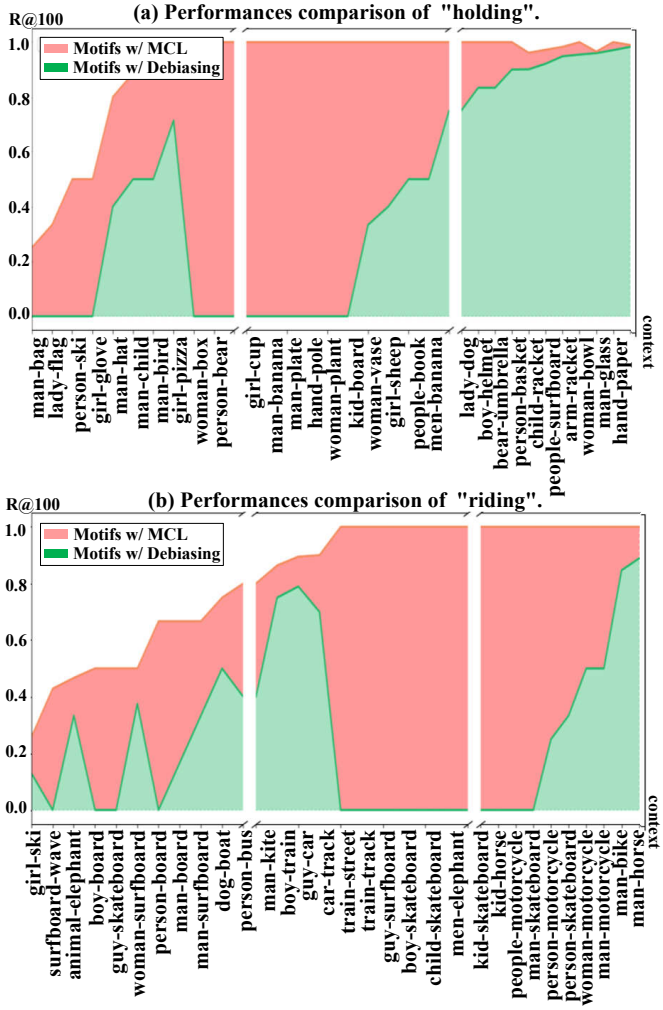

Fig. 5. **Effectiveness of MCL across contexts within the same predicate.** Motifs w/ MCL achieves more balanced predictions across different types of contexts than the Motifs w/ Debiasing.

various factors within them, i.e., the number of prototypes in CPC (Tab. VI) and the Memory Size of BPM (Tab. VII).

Effectiveness of the Designed Components. To investigate the effectiveness of each component of MCL, we conduct component-wise experiments by gradually removing them from the Motifs w/ MCL (i.e., $\mathbb{D}$) on the VG-SGG dataset under the PredCls task, as reported in Tab. V (i.e., $\mathbb{A}$-$\mathbb{D}$). Not surprisingly, all the components in MCL contribute to the final performance. To be specific, from $\mathbb{B}$, we observe the

TABLE IV
COMPARISON WITH SGG METHODS AT ZERO-SHOT RECALL (ZS-R@50/100) UNDER THREE SUB-TASKS ON THE VG-SGG DATASET.

Method	PredCls	SGCls	SGDet
	Zs-R@50/100	Zs-R@50/100	Zs-R@50/100
IETrans [14]$_{ECCV'22}$	2.5 / 3.7	0.1 / 0.1	0.0 / 0.0
SQUAT [33]$_{CVPR'23}$	2.9 / 3.8	1.2 / 1.8	0.5 / 1.0
Motifs [29]$_{CVPR'18}$	3.2 / 5.3	0.7 / 1.1	0.1 / 0.1
VCTree [47]$_{CVPR'19}$	3.3 / 5.5	1.2 / 2.1	0.3 / 0.7
Motifs-EBM [67]$_{CVPR'21}$	4.9 / -	1.3 / -	0.2 / -
Debiasing [1]$_{CVPR'19}$	4.5 / 6.6	1.4 / 0.9	1.2 / -
FC-SGG [68]$_{CVPR'21}$	7.9 / -	1.7 / -	0.9 / -
IS-GGT [69]$_{CVPR'23}$	8.3 / -	2.6 / -	1.3 / -
NARE [70]$_{CVPR'22}$	9.3 / 14.4	1.9 / 3.0	2.1 / 3.1
VCTree-TDE [25]$_{CVPR'20}$	14.3 / 17.6	3.2 / 4.0	2.6 / 3.2
Motifs-TDE [25]$_{CVPR'20}$	14.4 / 18.2	3.4 / 4.5	2.3 / 2.9
DeC [31]$_{TIP'23}$	15.8 / 19.5	3.2 / 4.1	2.3 / 3.1
GCA [32]$_{ICCV'21}$	18.5 / 20.4	3.8 / 4.4	1.7 / 2.5
PE-Net [20]$_{CVPR'23}$	17.2 / 20.9	5.3 / 6.5	2.3 / 3.6
MCL	**18.6 / 22.3**	**5.6 / 6.8**	**2.8 / 4.1**

superior performance over Motifs ($\mathbb{A}$) (e.g., 5.2% *vs.* 19.2% at Zs-R@100, 20.1% *vs.* 21.4% at mCR@100), verifying CPC's effectiveness in alleviating the concept-level imbalanced prediction problem. This can be attributed to its ability in capturing the variation and represent diverse concepts within the same predicate class. From $\mathbb{C}$, we observe that there is a significant improvement in all metrics after incorporating the CR (including $\mathcal{L}_e$, $\mathcal{L}_p$ and $\mathcal{L}_c$), demonstrating its effectiveness on improving model's unbiased relation recognition. We owe the effectiveness to both class-level/ instance-level/ concept-level dispersion encouraged by $\mathcal{L}_e$/ $\mathcal{L}_p$/ $\mathcal{L}_p$, which aid SGG models in effectively learning the Concept-guided Predicate Matching. Moreover, from $\mathbb{D}$, we observe that model's performance is further improved when CR and BPM are jointly utilized, highlighting their importance in assisting SGG models to learn concepts in a balanced manner, leading to robust and accurate relation recognition.

Analysis of amounts of Prototypes. To investigate how the amounts of prototypes P impact the model's performance, we conduct experiments with different M (i.e., $K = 1, 5, Ours, 10, 20$) choosing Motifs w/ MCL as the benchmark model, as shown in Tab. VI. Note that **Ours** denotes varying amounts of prototypes across predicates in CPC. From Tab. VI, we observe that the increase of P makes the model gradually capture the variation of diverse concepts within predicates, bringing improvements at R@100, mR@100, Zs-R@100, and mCR@100. As P continues to increase (i.e., larger than

TABLE V
ABLATION STUDIES FOR THE DESIGNED COMPONENTS OF MCL ON VG-SGG UNDER THE PREDCLS TASK. THE BASELINE MODEL IS MOTIFS.

Setup	Design	R@100	mR@100	F@100	Zs-R@100	mCR@100
𝔸	Motifs	**63.9** (+1.8)	15.5 (-26.4)	24.9 (-25.1)	5.2 (-16.5)	20.1 (-7.7)
𝔹	Motifs (w/ CPC)	59.4 (-2.7)	33.7 (-8.2)	43.0 (-7.0)	19.2 (-2.5)	21.4 (-6.4)
ℂ	Motifs (w/ CPC, BPM)	61.1 (-1.0)	40.2 (-1.7)	48.5 (-1.5)	21.5 (-0.2)	26.8 (-1.0)
𝔻	Motifs (w/ CPC, BPM, CR)	62.1	**41.9**	**50.0**	**21.7**	**27.8**

10), it becomes challenging for SGG models to effectively learn diverse concepts, leading to prototypes' redundancy and collapse and the performance degradation on all metrics. Ultimately, the experiments effectively demonstrate that the semantic complexity quantification-based CPC is more effective in assisting the model to understand and learn different concepts, compared to the traditional multi-prototype learning approach [49], [50].

Analysis of Memory Size. Here, we further explore the influence of different memory size M of BMP on model's performance. From Tab. VII, we have two observations: 1) Too large or too small memory size does not lead to a significant improvement in model's performance. 2) Our MCL is robust and not sensitive to selection of memory size M, indicating its general applicability. For instance, R@100, mR@100, Zs-R@100, mCR@100 get progressively improved with the increase of K, and peaked at $K = 64$ (i.e., R@100/ mR@100/ Zs-R@100/ mCR@100: 62.10%/ 41.94%/ 21.68%/ 27.76% with $K = 64$) before decreasing with larger K. Ultimately, we empirically figure out the best value for K as 64.

TABLE VI
ABLATION STUDY ON THE AMOUNTS PROTOTYPES K IN CPC. THE RESULTS ARE OBTAINED WITH THE MOTIFS AS THE BASELINE.

Setting	*PredCls*			
	R@100	mR@100	Zs-R@100	mCR@100
$K = 1$	60.24 (-1.86)	35.14 (-6.80)	20.16 (-1.52)	22.57 (-5.19)
$K = 5$	61.72 (-0.38)	38.73 (-3.21)	20.46 (-1.22)	24.61 (-3.15)
Ours	**62.10**	**41.94**	**21.68**	**27.76**
$K = 10$	61.70 (-0.40)	41.04 (-0.90)	21.01 (-0.67)	26.55 (-1.21)
$K = 20$	61.14 (-0.96)	40.63 (-1.31)	20.79 (-0.89)	26.25 (-1.51)

TABLE VII
ABLATION STUDY ON MEMORY SIZE M OF BPM. THE RESULTS ARE OBTAINED WITH THE MOTIFS AS THE BASELINE.

Setting	*PredCls*			
	R@100	mR@100	Zs-R@100	mCR@100
$M = 16$	61.27 (-0.83)	41.69 (-0.25)	21.20 (-0.48)	27.21 (-0.55)
$M = 32$	61.19 (-0.91)	41.58 (-0.36)	21.28 (-0.40)	26.92 (-0.84)
$\boldsymbol{K = 64}$	**62.10**	**41.94**	**21.68**	**27.76**
$M = 128$	61.75 (-0.35)	41.48 (-0.46)	21.50 (-0.18)	27.26 (-0.50)
$M = 256$	61.86 (-0.24)	41.20 (-0.74)	21.45 (-0.23)	27.34 (-0.42)

G. Qualitative Results

Here, we present qualitative results to intuitively validate that our MCL can effectively learn different concepts within predicates in a balanced manner. We demonstrate this through three aspects: The Attention Heat Map for model's prediction (Fig. 6), the t-SNE Scatter Map for relation feature distribution (Fig. 7), and Visualization of generated scene graphs (Fig. 8).

Visualization on Attention Heat Map. In Fig. 6, we visualize the prediction results with the attention heat maps of MCL w/ BPM (Fig. 6 (a)) and MCL w/o BPM (Fig. 6 (b)). From Fig. 6, we observe that the attention scores in MCL w/ BPM vary across different concepts, exhibiting higher values on their respective concepts P_1, P_2, P_3 (shown in Fig.6 (b), highlighted in red, yellow, and blue). Conversely, in MCL w/o BPM (shown in Fig. 6 (a)), the attention scores predominantly concentrate on the concept P_1. It powerfully demonstrates that our BPM helps differentiate among different concepts, resulting in a more balanced learning process across concepts within the same predicate.

Visualization on t-SNE Scatter Map. Additionally, we employ the t-SNE technique to visualize the feature distribution in model's latent space, as depicted in Fig. 7. In comparison to Motifs w/ Debiasing (Fig. 7 (a)), our MCL achieves higher predicate-level and concept-level discriminability in model's latent space. (Fig. 7 (b)). This improvement stems from two key aspects: On one hand, the MCL effectively matches relation features from different concepts to distinct concept-prototypes, enhancing the discriminability across different concepts. On the other hand, our MCL reduces the predicate-level overlap by enforcing larger distances between concepts with similar semantics but belonging to different predicate classes. These combined advancements in concept-level discriminability and predicate-level distinctiveness ensure the inter-class distinct and intra-class compact relation features in model's latent space.

Visualization on Scene Graphs. Furthermore, we make a comparison between scene graphs generated by Motifs (w/ Debiasing) (in green) and our method (in yellow) in Fig. 8. We observe that Motifs (w/ MCL) accurately infer relationships, such as "cat-near-chair" rather than "cat-sitting on-chair" in Fig. 8 (1) and "1-cow-eating-plant" as opposed to "1-cow-looking at-plant" in Fig. 8 (2). Furthermore, to validate MCL's compositional generability across contexts, we highlight few-shot relationships (in blue) involving rare/ uncommon concepts within images. We observe that our method can handle these few-shot instances, such as "pot-for-plant" in Fig. 8 (1), "2-cow-walking in-plant" in Fig. 8 (2), and "bear-sitting on-basket" in Fig. 8 (4). These results powerfully demonstrate that our MCL strengthens SGG model's compositional generability over rare/ uncommon concepts, ensuring balanced relation recognition across concepts within the same class.

V. CONCLUSION

This work proposes MCL, a novel and comprehensive framework, aiming at jointly addressing the challenges of (predicate, concept)-level imbalanced predictions in SGG.

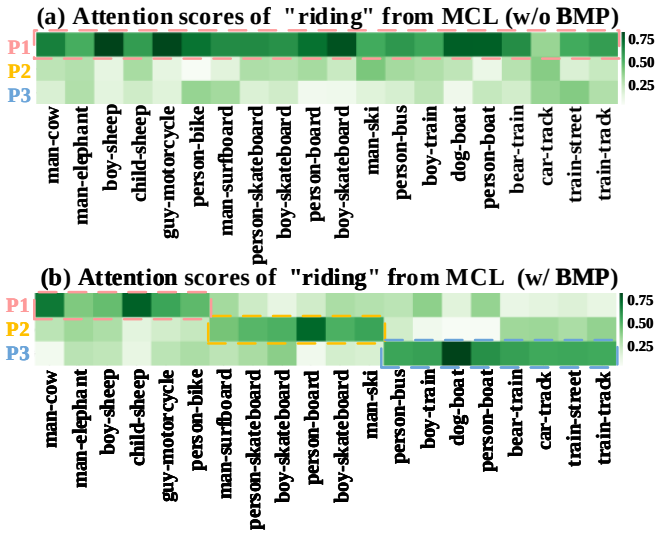

Fig. 6. **Attention scores for concepts matching.** In comparison with MCL w/o BPM, MCL w/ BPM effectively assigns samples with similar contexts to their corresponding concept-prototypes.

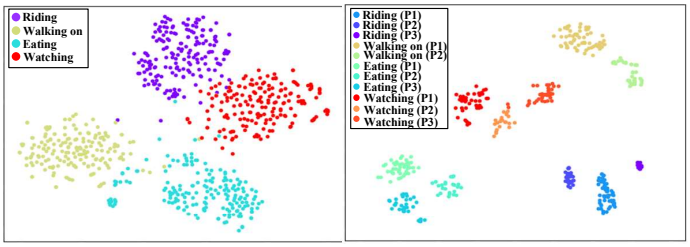

(a) Motifs w/ Debiasing. **(b) Motifs w/ MCL.**

Fig. 7. **The comparison of t-SNE visualization results.** Within the latent space of Motifs w/ MCL, samples belonging to the same predicate class exhibit a tendency to cluster around their respective concept-prototypes, acquiring inter-class distinct and intra-class compact relation features.

As a plug-and-play training framework, our MCL consistently enhances SGG models' predicate-level unbiased relation recognition capability, and their concept-level compositional generability across contexts. To demonstrate the effectiveness of MCL, we apply it to multiple SGG benchmark models and conduct experiments on both VG-SGG and OI-SGG datasets. The experimental results clearly demonstrate a significant improvement in performance compared to the benchmark models, thereby establishing a new state-of-the-art on both the VG-SGG and OI-SGG datasets. Furthermore, we conduct extensive experiments on zero-shot and few-shot relation recognition to showcase the compositional generability of our MCL.

REFERENCES

[1] Y. Cui, M. Jia, T. Lin, Y. Song, and S. J. Belongie, "Class-balanced loss based on effective number of samples," in *CVPR*, 2019. 1, 2, 7, 8, 9
[2] R. Herzig, A. Mendelson, L. Karlinsky, A. Arbelle, R. Feris, T. Darrell, and A. Globerson, "Incorporating structured representations into pretrained vision & language models using scene graphs," *CoRR*, 2023. 1
[3] Z. Wang, H. You, L. H. Li, A. Zareian, S. Park, Y. Liang, K. Chang, and S. Chang, "SGEITL: scene graph enhanced image-text learning for visual commonsense reasoning," in *AAAI*, 2022. 1
[4] B. Schroeder and S. Tripathi, "Structured query-based image retrieval using scene graphs," in *CVPR*, 2020. 1
[5] P. Zeng, L. Gao, X. Lyu, S. Jing, and J. Song, "Conceptual and syntactical cross-modal alignment with cross-level consistency for image-text matching," in *MM*, 2021. 1
[6] S. Yoon, W. Kang, S. Jeon, S. Lee, C. Han, J. Park, and E. Kim, "Image-to-image retrieval by learning similarity between scene graphs," in *AAAI*, 2021. 1
[7] P. Zeng, H. Zhang, L. Gao, J. Song, and H. T. Shen, "Video question answering with prior knowledge and object-sensitive learning," *TIP*, 2022. 1
[8] L. Gao, Y. Lei, P. Zeng, J. Song, M. Wang, and H. T. Shen, "Hierarchical representation network with auxiliary tasks for video captioning and video question answering," *TIP*, 2022. 1
[9] J. Song, L. Gao, F. Nie, H. T. Shen, Y. Yan, and N. Sebe, "Optimized graph learning using partial tags and multiple features for image and video annotation," *TIP.*, 2016. 1
[10] A. Farshad, Y. Yeganeh, Y. Chi, C. Shen, B. Ommer, and N. Navab, "Scenegenie: Scene graph guided diffusion models for image synthesis," *CoRR*, 2023. 1
[11] J. Johnson, A. Gupta, and L. Fei-Fei, "Image generation from scene graphs," in *CVPR*, 2018. 1
[12] S. Garg, H. Dhamo, A. Farshad, S. Musatian, N. Navab, and F. Tombari, "Unconditional scene graph generation," in *CVPR*, 2018. 1
[13] X. Dong, T. Gan, X. Song, J. Wu, Y. Cheng, and L. Nie, "Stacked hybrid-attention and group collaborative learning for unbiased scene graph generation," in *CVPR*, 2022. 1, 2, 7
[14] A. Zhang, Y. Yao, Q. Chen, W. Ji, Z. Liu, M. Sun, and T. Chua, "Fine-grained scene graph generation with data transfer," in *CoRR*, 2022. 1, 2, 6, 7, 9
[15] J. Yu, Y. Chai, Y. Wang, Y. Hu, and Q. Wu, "Cogtree: Cognition tree loss for unbiased scene graph generation," in *IJCAI*, 2021. 1, 2, 6
[16] Y. Guo, L. Gao, X. Wang, Y. Hu, X. Xu, X. Lu, H. T. Shen, and J. Song, "From general to specific: Informative scene graph generation via balance adjustment," in *ICCV*, 2021. 1, 2, 7
[17] R. Li, S. Zhang, B. Wan, and X. He, "Bipartite graph network with adaptive message passing for unbiased scene graph generation," in *CVPR*, 2021. 1, 2, 6, 7
[18] X. Lyu, L. Gao, Y. Guo, Z. Zhao, H. Huang, H. T. Shen, and J. Song, "Fine-grained predicates learning for scene graph generation," in *CVPR*, 2022. 1, 6
[19] X. Lyu, L. Gao, P. Zeng, H. T. Shen, and J. Song, "Adaptive fine-grained predicates learning for scene graph generation," *TPAMI*, 2023. 1, 2, 6, 8
[20] C. Zheng, X. Lyu, L. Gao, B. Dai, and J. Song, "Prototype-based embedding network for scene graph generation," *CVPR*, 2023. 2, 3, 6, 7, 8, 9
[21] Y. He, T. Ren, J. Tang, and G. Wu, "Heterogeneous learning for scene graph generation," in *MM*, 2022. 2, 6
[22] X. Li, L. Chen, G. Chen, Y. Feng, Y. Yang, and J. Xiao, "Decomposed prototype learning for few-shot scene graph generation," *CoRR*, 2023. 2
[23] Y. Li, X. Yang, X. Huang, Z. Ma, and C. Xu, "Zero-shot predicate prediction for scene graph parsing," in *TMM*, 2022. 2, 3
[24] B. A. Biswas and Q. Ji, "Probabilistic debiasing of scene graphs," in *CVPR*, 2023. 2, 7
[25] K. Tang, Y. Niu, J. Huang, J. Shi, and H. Zhang, "Unbiased scene graph generation from biased training," in *CVPR*, 2020. 2, 6, 7, 9
[26] L. Li, L. Chen, Y. Huang, Z. Zhang, S. Zhang, and J. Xiao, "The devil is in the labels: Noisy label correction for robust scene graph generation," in *CVPR*, 2022. 2, 6, 7
[27] C. Chen, Y. Zhan, B. Yu, L. Liu, Y. Luo, and B. Du, "Resistance training using prior bias: toward unbiased scene graph generation," in *AAAI*, 2022. 2, 3, 6, 7
[28] Y. Teng and L. Wang, "Structured sparse R-CNN for direct scene graph generation," in *CVPR*, 2022. 2
[29] R. Zellers, M. Yatskar, S. Thomson, and Y. Choi, "Neural motifs: Scene graph parsing with global context," in *CVPR*, 2018. 2, 3, 6, 7, 9
[30] Y. Yang and Z. Xu, "Rethinking the value of labels for improving class-imbalanced learning," in *NeurIPS*, 2020. 2
[31] T. He, L. Gao, J. Song, J. Cai, and Y. Li, "Semantic compositional learning for low-shot scene graph generation," in *CoRR*, 2021. 2, 7, 9
[32] K. Boris, de Vries Harm, C. Cătălina, T. G. W, C. Aaron, and B. Eugene, "Generative compositional augmentations for scene graph prediction," in *ICCV*, 2021. 2, 7, 9
[33] D. Jung, S. Kim, W. H. Kim, and M. Cho, "Devil's on the edges: Selective quad attention for scene graph generation," in *CVPR*, 2023. 2, 3, 7, 9

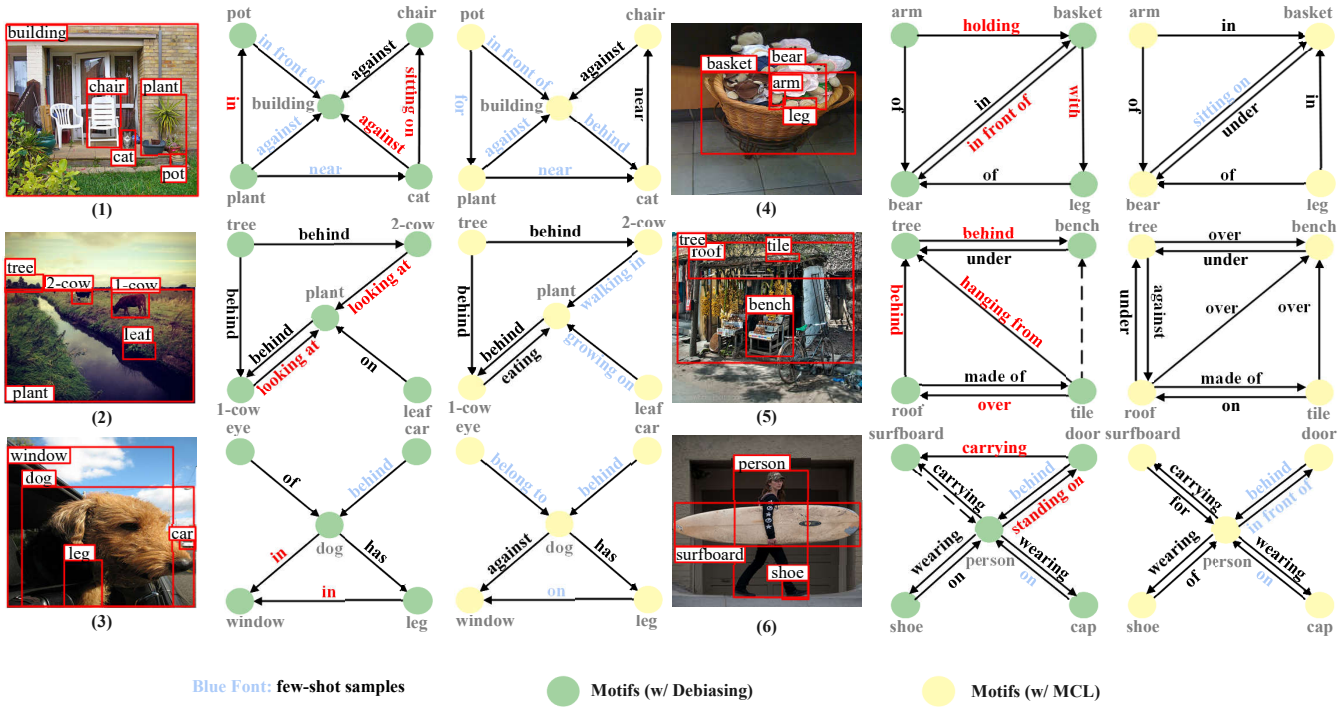

Fig. 8. **Scene graphs generated by Motifs (w/ Debiasing), and Motifs (w/ MCL) under the PredCls task.** Motifs (w/ MCL) are more faithful in describing few-shot instances than Motifs (w/ Debiasing). For clarity, we omit some relationships.

[34] A. Okazawa, "Interclass prototype relation for few-shot segmentation," in *ECCV*, 2022. 3

[35] L. Xingchen, C. Long, C. Guikun, F. Yinfu, Y. Yi, and X. Jun, "Decomposed prototype learning for few-shot scene graph generation," *CoRR*, 2023. 3

[36] H. Lee, M. Lee, and N. Kwak, "Few-shot object detection by attending to per-sample-prototype." in *WACV*, 2022. 3

[37] Q. Sanqing, C. Guang, Z. Jing, L. Zhijun, H. Wei, and T. Dacheng, "Bmd: A general class-balanced multicentric dynamic prototype strategy for source-free domain adaptation," in *ECCV*, 2022. 3

[38] H. Lin, Y. Zhang, Z. Qiu, S. Niu, C. Gan, Y. Liu, and M. Tan, "Prototype-guided continual adaptation for class-incremental unsupervised domain adaptation," in *ECCV*, 2022. 3

[39] B. Sergey, S. Adam, B. Matthew, W. Daan, and L. Timothy, "Meta-learning with memory-augmented neural networks," *JMLR*, 2016. 3

[40] L. Zhu and Y. Yang, "Inflated episodic memory with region self-attention for long-tailed visual recognition," in *CVPR*, 2020. 3

[41] L. Minhyeok, C. Suhwan, L. Seunghoon, P. Chaewon, and L. Sangyoun, "Unsupervised video object segmentation via prototype memory network," in *WACV*, 2023. 3

[42] A. Inigo, S. Alberto, F. David, M. Luis, and M. A. C, "Semi-supervised semantic segmentation with pixel-level contrastive learning from a class-wise memory bank," in *ICCV*, 2021. 3

[43] L. Zhao, X. Lyu, J. Song, and L. Gao, "Guesswhich? visual dialog with attentive memory network," *PR*, 2021. 3

[44] Y. Deng, Y. Li, Y. Zhang, X. Xiang, J. Wang, J. Chen, and J. Ma, "Hierarchical memory learning for fine-grained scene graph generation," in *ECCV*, 2022. 3, 6, 7

[45] J. Pennington, R. Socher, and C. D. Manning, "Glove: Global vectors for word representation," in *ACL*, 2014. 3

[46] J. Yang, J. Lu, S. Lee, D. Batra, and D. Parikh, "Graph R-CNN for scene graph generation," in *ECCV*, 2018. 3, 7

[47] K. Tang, H. Zhang, B. Wu, W. Luo, and W. Liu, "Learning to compose dynamic tree structures for visual contexts," in *CVPR*, 2019. 3, 6, 7, 9

[48] A. Vaswani, N. Shazeer, N. Parmar, J. Uszkoreit, L. Jones, A. N. Gomez, L. Kaiser, and I. Polosukhin, "Attention is all you need," in *NeurIPS*, 2017. 3, 5, 7

[49] A. Sablayrolles, M. Douze, C. Schmid, and H. Jégou, "Spreading vectors for similarity search," in *ICLR*, 2019. 4, 6, 10

[50] H. Guo, F. Xie, F. K. Soong, X. Wu, and H. Meng, "A multi-stage multi-codebook vq-vae approach to high-performance neural tts," in *IS*, 2022. 4, 6, 10

[51] J. Zhang, F. Zhan, C. Theobalt, and S. Lu, "Regularized vector quantization for tokenized image synthesis," in *CVPR*, 2023. 4, 6

[52] X. Zhu, J. Song, L. Gao, X. Gu, and H. T. Shen, "Revisiting multi-codebook quantization," *TIP*, 2023. 4, 6

[53] S. Yan, C. Shen, Z. Jin, J. Huang, R. Jiang, Y. Chen, and X. Hua, "PCPL: predicate-correlation perception learning for unbiased scene graph generation," in *MM*, 2020. 6

[54] C. Zheng, X. Lyu, Y. Guo, P. Zeng, J. Song, and L. Gao, "Learning to generate scene graph from head to tail," in *ICME*, 2022. 6

[55] X. Lin, C. Ding, J. Zhang, Y. Zhan, and D. Tao, "Ru-net: Regularized unrolling network for scene graph generation," in *CVPR*, 2022. 6, 7

[56] R. Krishna, Y. Zhu, O. Groth, J. Johnson, K. Hata, J. Kravitz, S. Chen, Y. Kalantidis, L.-J. Li, D. A. Shamma *et al.*, "Visual genome: Connecting language and vision using crowdsourced dense image annotations," *IJCV*, 2017. 6

[57] A. Kuznetsova, H. Rom, N. Alldrin, J. Uijlings, I. Krasin, J. Pont-Tuset, S. Kamali, S. Popov, M. Malloci, A. Kolesnikov *et al.*, "The open images dataset v4: Unified image classification, object detection, and visual relationship detection at scale," *IJCV*, 2020. 6

[58] K. Tang, "A scene graph generation codebase in pytorch," 2020, https://github.com/KaihuaTang/Scene-Graph-Benchmark.pytorch. 6

[59] M. Chen, X. Lyu, Y. Guo, J. Liu, L. Gao, and J. Song, "Multi-scale graph attention network for scene graph generation," in *ICME*, 2022. 6

[60] S. Ren, K. He, R. B. Girshick, and J. Sun, "Faster R-CNN: towards real-time object detection with region proposal networks," in *TPAMI*, 2017. 6

[61] W. Li, H. Zhang, Q. Bai, G. Zhao, N. Jiang, and X. Yuan, "Ppdl: Predicate probability distribution based loss for unbiased scene graph generation," in *CVPR*, 2022. 7

[62] X. Lin, C. Ding, J. Zeng, and D. Tao, "Gps-net: Graph property sensing network for scene graph generation," in *CVPR*, 2020. 7

[63] X. Han, X. Song, X. Dong, Y. Wei, M. Liu, and L. Nie, "Dbiased-p: Dual-biased predicate predictor for unbiased scene graph generation," in *TMM*, 2022. 7

[64] L. Tao, L. Mi, N. Li, X. Cheng, Y. Hu, and Z. Chen, "Predicate correlation learning for scene graph generation," in *TIP*, 2022. 7

[65] Y. Cong, M. Y. Yang, and B. Rosenhahn, "Reltr: Relation transformer for scene graph generation," *TPAMI*, 2022. 7

[66] X. Lin, C. Ding, Y. Zhan, Z. Li, and D. Tao, "Hl-net: Heterophily learning network for scene graph generation," in *CVPR*, 2022. 7
[67] M. Suhail, A. Mittal, B. Siddiquie, C. Broaddus, J. Eledath, G. G. Medioni, and L. Sigal, "Energy-based learning for scene graph generation," in *CVPR*, 2021. 8, 9
[68] L. Hengyue, Y. Ning, M. Masood, and B. Bir, "Fully convolutional scene graph generation," in *CVPR*, 2021. 9
[69] S. Kundu and S. N. Aakur, "Is-ggt: Iterative scene graph generation with generative transformers," in *ICCV*, 2021. 9
[70] A. Goel, B. Fernando, F. Keller, and H. Bilen, "Not all relations are equal: Mining informative labels for scene graph generation," in *CVPR*, 2022. 9